

In-flight Diagnostics in *LISA Pathfinder*

A. Lobo^{*,†}, M. Nofrarias[†], J. Ramos–Castro^{**}, J. Sanjuan[†], A. Conchillo[†],
J.A. Ortega[†], X. Xirgu[†], H. Araujo[‡], C. Boatella[†], M. Chmeissani[§], C.
Grimani[¶], C. Puigdemengoles[§], P. Wass[‡], E. García-Berro^{**}, S. García^{||}, L.M.
Martínez^{||} and G. Montero^{||}

^{*}*Instituto de Ciencias del Espacio (ICE), Barcelona, Spain*

[†]*Institut d'Estudis Espacials de Catalunya (IEEC), Barcelona, Spain*

^{**}*Universitat Politècnica de Catalunya (UPC), Barcelona, Spain*

[‡]*Imperial College of London (UK)*

[§]*Institut de Física d'Altes Energies (IFAE), Barcelona, Spain*

[¶]*Università di Urbino and INFN (Italy)*

^{||}*Atipic, Parc Tecnològic del Vallés, Barcelona, Spain*

Abstract. LISA PathFinder (LPF) will be flown with the objective to test in space key technologies for LISA. However its sensitivity goals are, for good reason, one order of magnitude less than those which LISA will have to meet, both in drag-free and optical metrology requirements, and in the observation frequency band. While the expected success of LPF will of course be of itself a major step forward to LISA, one might not forget that a further improvement by an order of magnitude in performance will still be needed. Clues for the last leap are to be derived from proper disentanglement of the various sources of noise which contribute to the total noise, as measured in flight during the PathFinder mission. This paper describes the principles, workings and requirements of one of the key tools to serve the above objective: the diagnostics subsystem. This consists in sets of temperature, magnetic field, and particle counter sensors, together with generators of controlled thermal and magnetic perturbations. At least during the commissioning phase, the latter will be used to identify *feed-through* coefficients between diagnostics sensor readings and associated actual noise contributions. A brief progress report of the current state of development of the diagnostics subsystem will be given as well.

Keywords: Gravity waves, LISA, LISA Pathfinder, diagnostics

PACS: 04.80.Nn, 95.55.Ym, 04.30.Nk

1. INTRODUCTION

LISA (Laser Interferometer Space Antenna), the joint ESA–NASA mission to place a Gravitational Wave (GW) detector in heliocentric orbit, is scheduled to fly within the next decade. The main objective of LISA is to observe GWs in a frequency band around 1 mHz, where many interesting sources are expected, but where earth based antennas are (by far) not sensitive to: many galactic binaries, massive black holes in distant galaxies and (perhaps) primeval GWs are amongst the signals LISA is expected to sight, at a minimum. LISA will measure ambient GW induced phase shifts in beams of laser light bouncing back and forth between freely falling test masses. According to basic theoretical principles (see e.g. [1]), this requires the nominal distance between the test masses to be of the order of $c/4\nu$, where ν is the frequency of the incoming GW and c is the speed of light. For $\nu \sim 1$ mHz this gives an arm length of a few million km. For LISA, 5×10^6 km has been baselined, and the mission is defined as a formation of three

spacecraft in a triangular configuration, 5×10^6 km to the side [2]. For this, a heliocentric orbit, 1 AU from the Sun, is foreseen.

The key concept for LISA to work is to ensure that the test masses are in nominal *free fall*, i.e., that they follow the geodesics of the local gravitational field. GWs of a given frequency then show up in the detector as *differential accelerations* between the test masses, at that frequency. This is why the sensitivity requirement for LISA is commonly stated in terms of relative acceleration noise. The current baseline is

$$S_{\Delta a}^{1/2}(\nu) = 3 \times 10^{-15} \left[1 + \left(\frac{\nu}{3 \text{ mHz}} \right)^2 \right] \text{ m s}^{-2} \text{ Hz}^{-1/2}, \quad 10^{-4} \text{ Hz} \leq \nu \leq 10^{-1} \text{ Hz} \quad (1)$$

This is a rather formidable requirement: picometre interferometry will be needed, and an extremely quiet environment for the test masses must be maintained. The latter is provided by a so called *drag-free* subsystem, which consists in a high precision test mass position sensing device, called *Gravitational Reference Sensor* (GRS), working in combination with a set of micro-thrusters which keep the spacecraft in orbit *following* the test masses.

The European Space Agency (ESA) has decided to launch a previous technology demonstrator to check in flight the feasibility issues of LISA. The mission is called LISA PathFinder (LPF), and is scheduled fly in 2009. Seven European countries participate in this mission.

The payload on board LPF is the *LISA Technology Package* (LTP), and includes several subsystems and interfaces, both amongst them and with the space platform itself, whose rigorous control is part of the experiment. The main purpose of the LTP is to test in space the key technologies for LISA. The concept is to use only two freely floating masses, and to follow their evolutions in a reduced size configuration: a LISA arm is squeezed from 5 million kilometres to about 30 centimetres, and a single spacecraft hosts both test masses, where drag-free and interferometry is implemented. In addition, a relaxed sensitivity requirement is adopted for LPF:

$$S_{\Delta a}^{1/2}(\nu) = 3 \times 10^{-14} \left[1 + \left(\frac{\nu}{3 \text{ mHz}} \right)^2 \right] \text{ m s}^{-2} \text{ Hz}^{-1/2}, \quad 1 \text{ mHz} \leq \nu \leq 30 \text{ mHz} \quad (2)$$

which is an order of magnitude below that of LISA, both in spectral density magnitude and in bandwidth.

One of the subsystems of the LTP is the so called *Data and Diagnostics Subsystem* (DDS), which consists in a series of items intended to monitor various factors of disturbance inside the payload. The purpose of these instruments is to provide information to split up the total system readout noise into different components, with the the goal of both diagnosing LTP performance, and guiding the search for the final sensitivity leap from equation (2) to (1). In addition, the DDS also provides the *Data Management Unit* (DMU), with several control and feedback functions, and on-board data analysis duties.

In the following pages we briefly review the motivation, significance and current state of development of the LTP DDS.

2. DIAGNOSTICS ELEMENTS

Three types of disturbances have been identified which need to be diagnosed in the LTP:

- Temperature fluctuations
- Magnetic fluctuations
- Incident fluxes of charged particles

A quantitative assessment of the actual contribution of each of these items to the total system noise requires not only to measure them but also knowledge of *transfer functions*. The latter provide the relationship between e.g. a temperature change and the associated system readout —normally in frequency domain. Such transfer functions are determined on the basis of in-flight experiments, which consist in measuring the effect of artificially induced perturbations on the system response. Controlled perturbations are applied by means of *heaters* and *magnetic coils* at suitable locations and with suitable properties. These are also part of the DDS.

2.1. Noise debugging philosophy

Let α be a controlled disturbance applied to the system. In practice, α will be a thermal gradient or a magnetic field and magnetic field gradient. It is expedient that α be a *coherent* signal, as this will make its identification in the readout data stream easier. Let $y(t; \alpha)$ be the instrumental response data stream —we leave it generic, as it can be phasemeter data, force on the test masses, or some other suitable magnitude. Using $y(t; \alpha)$, we calculate the *feedthrough* coefficient

$$F = \frac{\partial y}{\partial \alpha} \quad (3)$$

Normally, α will be strong enough that it can be unambiguously detected in the output data, $y(t; \alpha)$. Actually, the requirement is that it be seen with a SNR of 50 [4]. The idea is to extrapolate the value of the *feedthrough* coefficient F to the weaker disturbance regime prevailing during science mode mission operation, so that “ α -meter” readings (i.e., thermometers and magnetometers readings) can be translated into y -noise by multiplication by F .

With such operation, we can evaluate the contributions of magnetic and temperature fluctuations noise to the total LTP noise budget. In addition, we know the sources of those contributions —since they are provided by the magnetometers’ and thermometers’ readings. This is essential information to determine the line of improvement of system design in view to improve the LTP sensitivity towards the more demanding LISA goal, eq. (1). This is the reason why the LTP Diagnostics is such a necessary subsystem: it would surely be less relevant should LPF be the final mission, i.e., with no further projection into LISA.

The just described schematics is basically conceptual. However, its practical implementation has a number of complications which need to be thoroughly worked on to make it useful. For example, there are many thermometers measuring the effect of sev-

eral heaters. Hence we typically have a *multivariate problem*, with all its added nuances and technical difficulties —see Miquel Nofrarias *et al.*, also in this volume.

2.2. Thermal diagnostics

Thermal gradients are a major source of concern since they affect almost every component of the LTP. In the GRS, where the test masses are placed inside a vacuum enclosure, *radiation pressure* and *radiometer effects* have been identified as the major sources of temperature fluctuation noise —see [3] for a comprehensive discussion. These can be quantified and reliably modeled. The optical elements in the Optical Metrology System (OMS) are also affected by random temperature gradients, but their impact on the readout is much more elusive to detailed modeling in this case.

The top level Science Requirements [4] establish that temperature fluctuations noise should account for 10 % of the total instrument noise budget, at most. This sets a limit on acceptable temperature fluctuation noise at [3]

$$S_T^{1/2}(\nu) \leq 10^{-4} \text{ KHz}^{-1/2}, \quad 1 \text{ mHz} \leq \nu \leq 30 \text{ mHz} \quad (4)$$

The satellite design must of course comply with this limit. However, temperature measurements need to be taken at various strategic spots to gauge the actual temperature environment conditions. Resolution of such measurements must be more exigent, and $10^{-5} \text{ KHz}^{-1/2}$ is required for them, within the LTP measuring bandwidth (MBW). A total of 22 thermometers will be distributed across the LTP, close to the test masses inside the GRS, in the optical bench and in the LCA (LTP Core Assembly) mounting struts¹. The sensors have been chosen to be *thermistors*; the associated electronics has been designed, and prototypes built and tested [5]. They perform to full satisfaction —see Figure 1—, and are currently being submitted to *baking tests*. The reason for

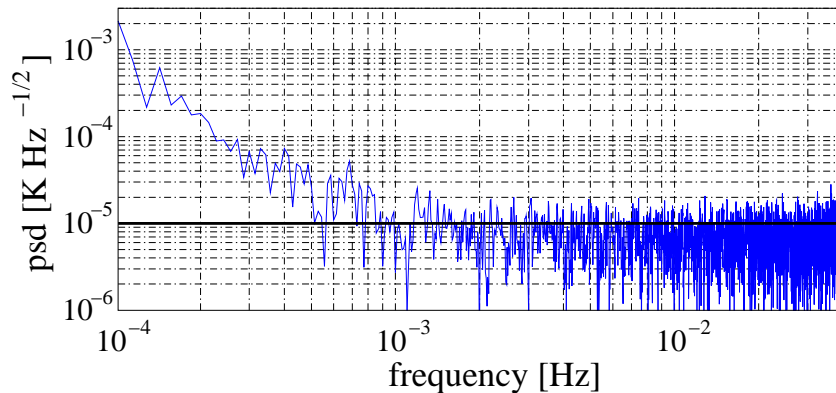


FIGURE 1. Power spectral density of thermistors plus their front-end electronics. Note that it is in the required level of $10^{-5} \text{ KHz}^{-1/2}$ throughout the MBW.

¹ They are carbon fibre beams with titanium braces which keep the LCA tied to the spacecraft structure.

such tests is that the entire GRS structure, including of course temperature sensors and wirings, will be heated up in order to inhibit outgassing inside it.

But, once the temperature readings are given, next question is: how do we extract useful information from them? We clearly need to know the relationship between temperature and system readout. As mentioned in the previous section, thermal control signals must be applied to the LTP, then measure its response. Details on this matter will be found in Miquel Nofrarias *et al.*, also in this volume.

2.3. Magnetic fluctuations

Each of the LTP test masses is a cube, 46 mm to the side, 1.96 kg of mass, and made of an alloy of 70 % gold and 30 % platinum. This has a very low magnetic susceptibility, $|\chi| \leq 10^{-5}$, and a very low remnant magnetic moment, too: $|\mathbf{m}_0| \leq 10^{-8} \text{ A m}^2$. Nevertheless, fluctuations of these magnitudes, as well as of environmental magnetic fields and gradients, will contribute to the system's overall noise. Just like temperature fluctuations, in-flight measurements of magnetic disturbances are necessary for a thorough assessment of mission design, i.e., how much *magnetic noise* is present in the readout.

Magnetic diagnostics pose significant measurement problems. Indeed, sensitive magnetometers make use of high susceptibility magnetic core materials, which may therefore not get too close to the TMs, hence field value extrapolations are required to estimate their value at the TMs. Algorithms for this are currently under investigation [6], and are at present based on *offline* statistical procedures. Error margins are in the order of 10 % to 40 %, which is quite good for the difficult magnetometer configuration which has been baselined at system level: four *fluxgate* magnetometers at distances in excess of 15 cm to the closest TM. Further refinements are being worked on, and improvements are shortly expected.

Magnetic fields have a distinctive feature: this is the fact that, so long as the TM susceptibility is non-zero, magnetisation on the TMs is induced, hence a force on them. If the magnetic field is \mathbf{B} then the force is given by

$$\mathbf{F} = \left\langle \left[\left(\mathbf{m}_0 + \frac{\chi V}{\mu_0} \mathbf{B} \right) \cdot \nabla \right] \mathbf{B} \right\rangle \quad (5)$$

where V is the test mass volume, and $\langle - \rangle$ stands for volume average within the test mass. Equation (5) shows that magnetic field intensity relates *non-linearly* to the associated force, and this has two important consequences: first, magnetic field and gradient *DC* components need to be properly monitored, as they couple to each other's fluctuating components; and second, high frequency magnetic field fluctuations result in *DC* —or low frequency— forces because of the quadratic dependence of \mathbf{F} on \mathbf{B} .

Magnetic diagnostics also include the concept of controlled generation of magnetic fields —see section 2.1 above. This is provided by magnetic induction coils (one per TM) which produce *non-homogeneous* magnetic fields in the vicinity of the TMs. The quadratic nature of the magnetic force shown by equation (5) results in a two-frequency response to a one-frequency input: a sinusoidal signal of frequency ω in the coil generates a response at the same frequency which is proportional to the TM remnant

magnetic moment \mathbf{m}_0 , plus a signal at 2ω , proportional to the TM susceptibility, χ . This means that \mathbf{m}_0 and χ can both be re-measured in flight, and that magnetic noise debugging can proceed thereafter, as explained above.

2.4. Radiation monitor

Cosmic rays and certain solar events contain ionising particles which will hit the LTP in flight, thus causing spurious signals in the GRS. These particles are mostly protons, with 10 % or less of He nuclei, and a tiny fraction of heavier nuclei, electrons and solar ions. Charging rates and the properties of noise caused by charging vary depending on whether the particle flux comes from Galactic Cosmic Rays (GCR) or is augmented by Solar Energetic Particles (SEP). The reason is that the two types of radiation present different energy spectra. Although average charging rates are detected by a dedicated measurement provided by the GRS, temporal *fluctuations* of the GCR flux and SEP can contaminate the data. A particle counter is thus necessary to provide correlations between the flux of energetic particles and the instantaneous charging rates observed in the test masses. In addition, the device must have the ability to distinguish SEP events from GCRs, and this consequently means it needs to determine the *energy spectra* of the detected particles. Finally, not all charged particles hitting the satellite structure will make it to the test masses, as that structure itself has a certain *stopping power*. The particle counter must only be triggered by those particles having enough energy to reach the TMs, hence it must be properly *shielded*. Simulation work indicates that only ions with energies larger than ~ 100 MeV should be counted [7]. The particle counter together with the above added capabilities is known as Radiation Monitor (RM). Contrary to the previous diagnostics, the RM does not require in-flight calibration.

An RM prototype has been designed and built in IFAE (Barcelona), with essential collaboration with Imperial College (London) and the University of Urbino [8]. The design concept consists in a pair of PIN diodes in telescopic configuration; incoming ionising particles generate charge in each PIN diode which is measured by dedicated electronics. This charge deposit provides a measurement of the incoming particle's energy, but it cannot tell e.g. protons from photons. Coincident events in both PIN diodes exclude photons, so spectral analysis is done on coincidence data to select only charged particle impacts, and to resolve SEP from GCR events. The significance of RM data is not based on individual events but on statistics of longer data stretches.

A most important part of the RM is the *shielding* which protects the PIN diodes against impacts of particles with energies below 100 MeV. This has a cubic copper profile, with rounded vertices, some 6 mm thick. The RM has been thoroughly tested to ensure its workings under electronically generated impulses. It has also been submitted to laboratory proton beam irradiation at the Paul Scherrer Institute (PSI) in Switzerland, and the results are very satisfactory in general —see P. Wass *et al.*, also in this volume.

A concern raised by the PSI test was the possible activation of the copper shield under excess irradiation conditions. These are considered unlikely in Lagrange-L1, but alternatives will also be considered and analysed during the following test, with fully space qualified materials.

3. THE DATA MANAGEMENT UNIT (DMU)

The DMU is the LTP computer. It holds full control of the diagnostics elements, i.e., powers them on and off (according to function programmes), acquires data, and processes them. Additionally, a number of other LTP functions are also managed by the DMU. The DMU is however subordinated to the mission on-board computer (OBC).

The hardware of the DMU consists in three major electronic boards: the Power Distribution Unit (PDU), Data Acquisition Unit (DAU), and Data Processing Unit (DPU). However, each of these boards is *duplicated for redundancy*. The PDUs and the DPUs work in a hot-cold redundancy scheme, which means only one of these boards is on at any given time. The DAUs are instead both operative at all times, and tasks are strategically distributed between them to minimise losses in case one of them fails.

The software running in this machine has two major components: the *Boot Software* (BSW) and the *Application Software* (ASW). Writing of both pieces of software requires intensive interaction with several other mission partners, as a significant part of it interfaces with subsystems different from the DDS. Progress is good so far, and the developers team includes the industrial contractor personnel (NTE). Further details will be found in J.A. Ortega *et al.* report, also in this volume.

4. CONCLUSION

Shortly after the end of the LISA Symposium, the DDS went through a Delta-PDR (Preliminary Design Review) in July-2006, in which two items pending from the initial PDR (September 2005) were reviewed again. PDR will be closed after a number of actions are completed. Next landmark is the Critical Design Review (CDR), in a few months time. Hardware procurement and assembly will however start even before, as there are a number of items in which no changes can be reasonably expected. We are confident that conditions look good for a successful completion of the DDS, a very important mission subsystem, of course framed within a global mission progress success.

Acknowledgement: We thank Ministerio de Educación y Ciencia for support under contract ESP2004-01647.

REFERENCES

1. J.A. Lobo, *Classical and Quantum Gravity* **9**, 1385 (1992).
2. A. Hammesfahr *et al.*, *LISA, a Cornerstone mission for the observation of Gravitational Waves*, ESA document ESA-SCI(2000)11 (2000).
3. J.A. Lobo, M. Nofrarias, J. Ramos-Castro, J. Sanjuan, *Class. Quant. Grav.* **23**, 5177-5193 (2006).
4. S. Vitale *et al.*, *Science Requirements and Top-level Architecture Definition for the Lisa Technology Package (LTP) on Board LISA PathFinder*, LPF document LTPA-UTN-ScRD-Iss003-Rev1.
5. J. Ramos-Castro and J. Sanjuan, *DDS Thermal Diagnostic Prototype Design*, Technical Report S2-UPC-DDD-3001, UPC-IEEC (2005).
6. S. García, and L.M. Martínez, *Reconstruction of the Magnetic Field and Gradient on Test Masses of LISA PathFinder*, Technical Report S2-IEEC-TN-3024, Atipic-IEEC (2006).
7. H.M. Araújo, P. Wass, D. Shaul, G. Rochester, T.J. Sumner, *Astrop. Phys.* **22**, 451-469 (2005).
8. C. Boatella, M. Chmeissani, C. Puigdemonges, *LISA PathFinder Radiation Monitor Design*, Technical Report S2-IFAE-DDD-3002, IFAE-IEEC (2006).